JOURNAL OF CHEMOMETRICS
J. Chemometrics 2002; **16**: 28–40

Constrained least squares methods for estimating reaction rate constants from spectroscopic data

Sabina Bijlsma[1], Hans F. M. Boelens[2], Huub C. J. Hoefsloot[3] and Age K. Smilde[2]*
[1]TNO Nutrition and Food Research, Utrechtseweg 48, NL-3700 AJ Zeist, The Netherlands
[2]Process Analysis and Chemometrics, Department of Chemical Engineering, University of Amsterdam, Nieuwe Achtergracht 166, NL-1018 WV Amsterdam, The Netherlands
[3]Polymer and Process Systems, Department of Chemical Engineering, University of Amsterdam, Nieuwe Achtergracht 166, NL-1018 WV Amsterdam, The Netherlands

Received 9 May 2000; Revised 10 November 2000; Accepted 14 November 2000

Model errors, experimental errors and instrumental noise influence the accuracy of reaction rate constant estimates obtained from spectral data recorded in time during a chemical reaction. In order to improve the accuracy, which can be divided into the precision and bias of reaction rate constant estimates, constraints can be used within the estimation procedure. The impact of different constraints on the accuracy of reaction rate constant estimates has been investigated using classical curve resolution (CCR). Different types of constraints can be used in CCR. For example, if pure spectra of reacting absorbing species are known in advance, this knowledge can be used explicitly. Also, the fact that pure spectra of reacting absorbing species are non-negative is a constraint that can be used in CCR. Experimental data have been obtained from UV-vis spectra taken in time of a biochemical reaction. From the experimental data, reaction rate constants and pure spectra were estimated with and without implementation of constraints in CCR. Because only the precision of reaction rate constant estimates could be investigated using the experimental data, simulations were set up that were similar to the experimental data in order to additionally investigate the bias of reaction rate constant estimates. From the results of the simulated data it is concluded that the use of constraints does not result self-evidently in an improvement in the accuracy of rate constant estimates. Guidelines for using constraints are given. Copyright © 2002 John Wiley & Sons, Ltd.

KEYWORDS: constraints; reaction rate constants; UV-vis spectroscopy; curve resolution; accuracy

1. INTRODUCTION

Many methods are available which can be used to estimate reaction rate constants from spectral data of chemical reactions [1–18] (also S. Bijlsma *et al.*, submitted). Different techniques such as target testing (TT) [1], global analysis [2–4], Kalman filter [5,6], traditional curve-fitting (TCF)-based techniques [7–12], curve resolution [13–17] and three-way analysis [16,18,19] are used to obtain unknown reaction rate constants from spectral data of chemical reactions. All these methods except TCF are multivariate methods which can deal with the presence of spectral overlap.

Curve resolution [13,20] is a group of techniques based on the determination of qualitative information and the recovery of response profiles, e.g. time profiles. The traditional curve resolution techniques can be adapted in order to estimate pure spectra of reacting absorbing species and reaction rate constants from kinetic data simultaneously using specific kinetic model information. In that case the kinetic equations are used explicitly by the algorithm [14–17].

The accuracy of an estimated reaction rate constant can be divided into the precision and bias of the estimate. The accuracy of the reaction rate constant estimate decreases by increasing model errors, experimental errors and instrumental noise. Model errors, experimental errors and instrumental noise are always present. Examples of experimental errors are errors due to the start of the reaction, initial concentration errors of reactants at the start of the reaction and temperature fluctuations during the reaction. If a suitable kinetic model for the data is used and the Beer–Lambert law is valid, model errors can be kept small.

Possibly, the accuracy of reaction rate constant estimates can be improved by using constraints during the optimization procedure. In the literature, constraints such as unimodality of concentration profiles [21,22], closure [20,23], selectivity [21] and non-negativity of both concentration profiles and pure spectra [21,23] are used during optimization of the curve resolution model in order to improve the precision of parameter estimates. Often some of the pure spectra of the absorbing species involved in the chemical reactions of interest are known beforehand or easy

---

* Correspondence to: A. K. Smilde, Process Analysis and Chemometrics, Department of Chemical Engineering, University of Amsterdam, Nieuwe Achtergracht 166, NL-1018 WV Amsterdam, The Netherlands
E-mail: asmilde@its.chem.uva.nl

DOI:10.1002/cem.668

to measure. These pure spectra can be used as constraints in curve resolution techniques. In previous work [15,16] this approach appeared to be very useful, leading to more precise estimates of reaction rate constants. The property that pure spectra are always non-negative was also used as a constraint in previous work [12,15–17]. This constraint can be used in the fast non-negative least squares algorithm of Bro and de Jong [24].

The goal of this paper is to determine the impact of constraints in CCR on the accuracy of reaction rate constant estimates, to establish whether the use of constraints is always beneficial, and finally to define guidelines for the use of constraints. Also, the use of perfect *a priori* knowledge and imperfect *a priori* knowledge of the constraints is investigated. This paper reports a first systematic study on imposing constraints in algorithms for estimating reaction rate constants from spectral data.

A two-step biochemical reaction, of which the first step may be described by pseudo-first-order kinetics, has been monitored using UV-vis spectroscopy [25]. The severe overlap of the spectra of the reactant and product makes this data set especially suitable for investigating the application of constraints. In previous work [12, 17] the same experimental data were used in order to estimate the reaction rate constants involved using algorithms such classical curve resolution (CCR) [12, 17] and TCF [12]. In other work [15,16,19], experimental data from the same reaction were used to estimate the reaction rate constants of interest using CCR [15,16], weighted curve resolution (WCR) [16] and three-way analysis [16,19], although those data were obtained at a larger pH which resulted in other values for the reaction rate constants.

From the collected spectral data the reaction rate constants and the pure spectra of individual reacting absorbing species have been estimated simultaneously. CCR with and without constraints was used. Using the experimental data, only the precision of the reaction rate constant estimates could be investigated, because the true values for the reaction rate constants are unknown. Therefore simulations have been performed to investigate the bias of reaction rate constant estimates.

2. THEORY

2.1. Notation

Bold-face capital characters represent matrices and bold-face lower-case characters represent vectors. The superscript 'T' indicates the transpose, $\hat{\mathbf{X}}$ denotes the estimate of matrix **X**, and $\mathbf{X}^{-1}$ represents the inverse of matrix **X**.

2.2. The measurement model

Suppose matrix **A** ($M \times N$) contains a collection of spectra in time of a chemical reaction with M wavelengths, N time points and K reacting absorbing species. Matrix **A** can be decomposed as follows assuming the Beer–Lambert law [24]:

$$\mathbf{A} = \mathbf{D}\mathbf{F}^{\mathrm{T}} + \mathbf{E} \tag{1}$$

The matrices in Equation (1) have the following properties.

1. **D** ($M \times K$) contains the pure spectra of K reacting absorbing species stored in columns.
2. **F** ($N \times K$) contains the concentration profiles of K reacting absorbing species stored in columns.
3. **E** ($M \times N$) is a matrix of errors (model errors, experimental errors and instrumental noise).

In practice, **F** and **D** are both *unknown*. Sometimes a part of **D** (pure spectra of reacting absorbing species) is *known* in advance. If this is not the case, it is very often possible to measure pure spectra of reactants and products easily. However, obtaining the pure spectrum of an intermediate species can be a problem, because it is difficult to isolate. Matrix **F** is *unknown*, but a model for **F** (structure) is *known* if a suitable kinetic model for the chemical reaction of interest is *known*. Suppose the following reaction is considered:

$$\mathrm{U} + \mathrm{V} \xrightarrow{k_1} \mathrm{W} \xrightarrow{k_2} \mathrm{Y}$$

where k_1 is a pseudo-first-order reaction rate constant in min^{-1}. If pseudo-first-order kinetics can be assumed (large excess of species V) and k_2 is a first-order reaction rate constant also in min^{-1}, Equations (2)–(4) describe the concentration profiles of species U (reactant), species W (intermediate) and species Y (product) respectively:

$$C_{\mathrm{U},i} = C_{\mathrm{U},0}\mathrm{e}^{-k_1 t_i} \tag{2}$$

$$C_{\mathrm{W},i} = \frac{C_{\mathrm{U},0}k_1}{k_2 - k_1}(\mathrm{e}^{-k_1 t_i} - \mathrm{e}^{-k_2 t_i}) \tag{3}$$

$$C_{\mathrm{Y},i} = C_{\mathrm{U},0} - C_{\mathrm{U},i} - C_{\mathrm{W},i} \tag{4}$$

where $C_{\mathrm{U},0}$ is the initial concentration of species U, and $C_{\mathrm{U},i}$, $C_{\mathrm{W},i}$ and $C_{\mathrm{Y},i}$ are the concentrations of species U, species W and species Y at time t_i respectively. It is assumed that initially only reactant species U and V are present.

The first column of **F** can be represented by Equation (2). Hence matrix **F** can be reconstructed if the reaction rate constants are given a value. For first-order kinetics the decomposition of Equation (1) is unique apart from a permutation of the kinetic constants [26,27] (also A. K. Smilde *et al.*, submitted). Chemical knowledge is required to solve this permutation ambiguity.

2.3. Classical curve resolution (CCR)

An estimate of k_1, k_2 and **D** can be obtained simultaneously by minimization of the sum of squares (SSQ) of residuals defined in Equation (5) according to an alternating least squares scheme:

$$\mathrm{SSQ} = \sum_{m=1}^{M}\sum_{n=1}^{N} e_{mn}^2 \tag{5}$$

where the residual e_{mn} is the (m,n)th element of matrix **E** from Equation (1). In the Appendix the algorithm of CCR is listed.

2.4. Different types of constraints

Three constraints are used in which the measured pure spectra of reactant and/or product have been supplied to CCR. For each constraint the spectra of the compounds in matrix **D** that are *not* supplied to CCR and the values of k_1

and k_2 are still updated by the algorithm. In *constraint R* the pure spectrum of the reactant, which was measured for every individual batch, is supplied; in *constraint P* the pure spectrum of the reaction product measured is used; and in *constraint RP* the pure spectra of both the reactant and product are fixed.

Additionally, in the fourth *constraint NNLS* the ordinary least squares step of the CCR algorithm (see Appendix) that is used to determine the **D** matrix is changed into a non-negative least squares step [24].

2.5. Accuracy of reaction rate constant estimates

The accuracy of a parameter can be split into the precision and bias of the parameter according to

$$\underbrace{E(\hat{k}-k_{\text{true}})^2}_{\text{accuracy}} = \underbrace{E(\hat{k}-E(\hat{k}))^2}_{\text{precision}} + \underbrace{(E(\hat{k})-k_{\text{true}})^2}_{\text{bias}} \tag{6}$$

where E indicates the expectation operator. The accuracy, bias and precision of a parameter can be estimated by applying Equations (7)–(9) respectively

$$\text{accuracy} = \frac{1}{N}\sum_{n=1}^{N}(\hat{k}_n - k_{\text{true}})^2 \tag{7}$$

$$\text{bias} = (\bar{\hat{k}} - k_{\text{true}})^2 \tag{8}$$

$$\text{precision} = \frac{1}{N-1}\sum_{n=1}^{N}(\hat{k}_n - \bar{\hat{k}})^2 \tag{9}$$

where

$$\bar{\hat{k}} = \frac{1}{N}\sum_{n=1}^{N}\hat{k}_n, \quad n = 1,2,3,\ldots,N \tag{10}$$

Relative errors are reported according to

$$\text{relative error} = \frac{\sqrt{\text{accuracy}}}{\text{true value}} \times 100\% \tag{11}$$

3. EXPERIMENTAL

3.1. The biochemical reaction monitored

A two-step consecutive biochemical reaction was monitored using UV-vis spectroscopy [8,10,19]. In the first reaction step, 3-chlorophenylhydrazonopropane dinitrile (species U) reacts with a large excess of 2-mercaptoethanol (species V) into an intermediate adduct (species W). In the second step of the reaction, main product 3-chlorophenylhydrazonocyanoacetamide (species Y) and by-product ethylene sulphide (species Z) are created from the intermediate adduct by means of an intramolecular reaction. A detailed reaction mechanism can be found in an earlier paper [19].

3.2. Reagents and experimental set-up

The reagents, sample preparation and experimental set-up used were described in earlier papers [12, 17]. A 1.00 cm cuvette (Hellma Benelux) was filled with 2.5 ml of the reaction mixture containing 54 μmol l^{-1} of species U buffered with KH_2PO_4 (Acros, pro analysis 0.2 mol l^{-1}, pH 4.4). After reaching the reaction temperature of 25 °C, 10 μl of species V was added and data collection was started immediately. Every 10 s a spectrum of the reaction mixture was recorded for the wavelength range 300–500 nm. The reaction was monitored for 45 min. Four experiments were run per day. In total, 32 experiments were performed under the same conditions ($N = 32$).

A Hewlett Packard 8453 spectrophotometer with diode array detection was used to obtain spectra of the reaction mixture. The reaction temperature was kept constant using a water bath (Neslab) equipped with a thermocouple inside the cuvette as external temperature sensor.

3.3. Measured pure spectrum of reactant (species U) and product (species Y)

As an estimate of the pure spectrum of the reactant, the average of 21 blank corrected spectra was calculated. For each individual batch these 21 spectra were recorded before species V was added to the reactant. For all 32 batches these pure spectra of the reactant were calculated. The pure spectrum of the product is estimated by taking the average of 21 blank-corrected spectra of the reaction mixture after a reaction time of 8 h. The reaction constants as estimated by CCR show that the conversion after this time period is about 100%. At that time, only species V, species Y and species Z are present in the reaction mixture. Because species V and species Z both have no absorbances in the considered wavelength range, the calculated spectrum can be considered as the pure spectrum of the product. Only for two batches was this pure spectrum determined. Figure 1 shows the pure spectra of the reactant and product. It can be observed that the overlap between the two pure spectra shown is severe. This overlap makes this data set a nice example for testing the usefulness of applying constraints.

3.4. Data processing

The spectrum of the buffer solution was used as blank for all experiments described. The starting values for k_1 and k_2 in the CCR algorithm were set to 0.30 and 0.03 min^{-1} respectively. These starting values were chosen around the optimal values of the reaction rate constants obtained in previous papers [12, 17]. Using different starting values yielded similar results. An offset correction has been applied by subtracting the mean absorbance in the wavelength range 560–600 nm from all absorbances. Because of the low repeatability of the first recorded spectrum after the start of the reaction, this spectrum was not further used.

3.5. Simulations

The simulations were set up to ensure that the simulated spectra of the reaction mixture are very similar to the measured spectra during the batch experiments.

3.5.1. Set-up

1. The mean reaction rate constants $\bar{k}_1$(= 0.2396 min^{-1}) and $\bar{k}_2$ (=0.0266 min^{-1}) based on all individual reaction rate constant estimates for the experimental data were determined. These mean values were taken to be the ‘true’ values of the reaction rate constants throughout the simulations.
2. The concentration profiles in matrix **F** were reconstructed

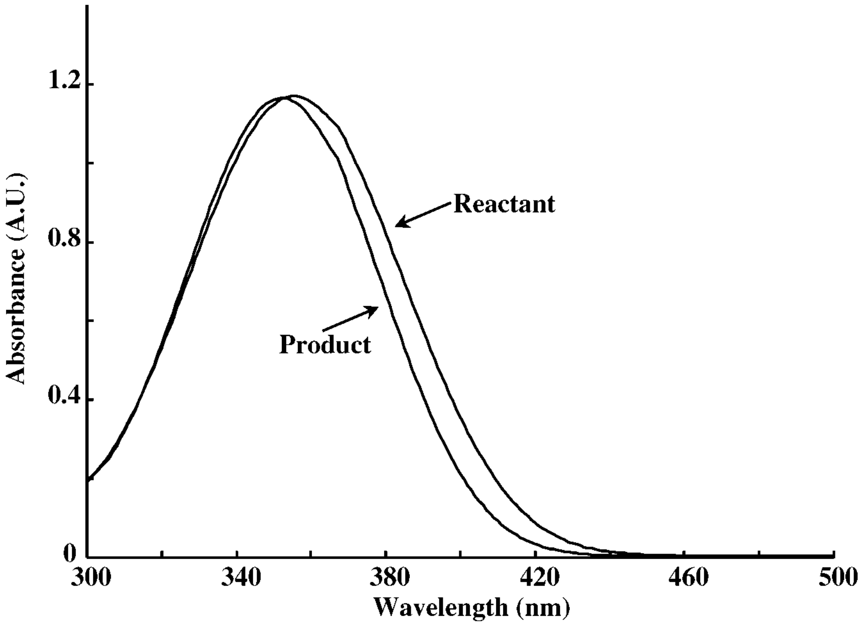

Figure 1. Averaged recorded pure spectra of reactant and product.

using $\bar{k}_1$ and $\bar{k}_2$ and setting the initial concentration of the reactant to 54 μmol l^{-1}.

3. The pure spectra estimated from a single batch using the CCR algorithm without constraints were taken as the 'true' pure spectra in the simulations (matrix **D**).
4. Using the equation $\mathbf{A} = \mathbf{D}\mathbf{F}^T$, the spectra of the reaction mixture in time were calculated (= matrix **A**).
5. To these 'true' spectra, normally distributed white noise was added. The sigma of the noise was taken to be a percentage of the maximum absorbance of the *first* simulated spectrum in matrix **A**. Two different noise levels, namely 0.2% and 2%, were selected. The level of 0.2% is approximately equal to the level of the instrumental noise. For each noise level, 500 instances of data matrix **A** were generated.

3.5.2. *Types of a priori knowledge*

When applying the constraints R, P or RP, two types of *a priori* knowledge were considered. Assuming perfect *a priori* knowledge, the 'true' pure spectra (see step 3 above) were imposed, and assuming imperfect *a priori* knowledge, these 'true' pure spectra were disturbed. This disturbance consisted either of white noise or of (realistic) shape differences. The level of the disturbing white noise was always selected equal to the noise level of the simulated spectra of the reaction mixture.

The procedure used to determine the realistic shape differences for the reactant spectrum is the following. As already mentioned, 32 estimates of the pure spectra of the reactant are available. The difference spectra of these estimates were calculated with respect to the pure spectrum of the reactant for the specific batch run used to generate the simulation model. Of the 31 difference spectra obtained in this way, the largest was used to disturb the pure spectrum of the reactant that was supplied to the CCR algorihm. Even larger, and therefore non-realistic, shape differences were introduced by first multiplying the previously calculated difference spectrum by a factor of 10 before adding it to the pure spectrum of the reactant.

The available data set to determine realistic shape differences for the product spectrum consists of only two estimated pure spectra of the product. The difference spectrum of the two spectra was calculated and added to the pure spectrum of the product. Again a larger shape difference was also introduced by multiplying the difference spectrum by a factor of 10 before addition to the pure spectrum of the reactant.

2 (reactant) and 3 (product) show the imposed pure spectra in the case of no shape differences, of realistic shape differences and of large shape differences.

4. RESULTS AND DISCUSSION

4.1. Experiments

4.1.1. *Precision of reaction rate constant estimates*

The CCR algorithm with and without constraints implemented has been used to estimate the reaction rate constants from the pseudo-first-order data set described. The reaction rate constant estimates from all individual batches are shown in Figure 4. From this figure the following can be observed.

1. The use of constraint R (Figure 4B) has led to a slightly poorer precision of the k_2 estimates compared to the k_2 estimates using no constraints (Figure 4A). The precision of the k_1 estimates is the same.
2. The use of constraint RP (Figure 4C) and constraint P (Figure 4D) has led to the best precision of the k_2 estimates compared to the results for no constraints (Figure 4A) and constraint R (Figure 4B). The precision of the k_1 estimates is again not affected by imposing constraints.
3. There is a small systematic difference between the reaction rate constant estimates for k_2 obtained with unconstrained

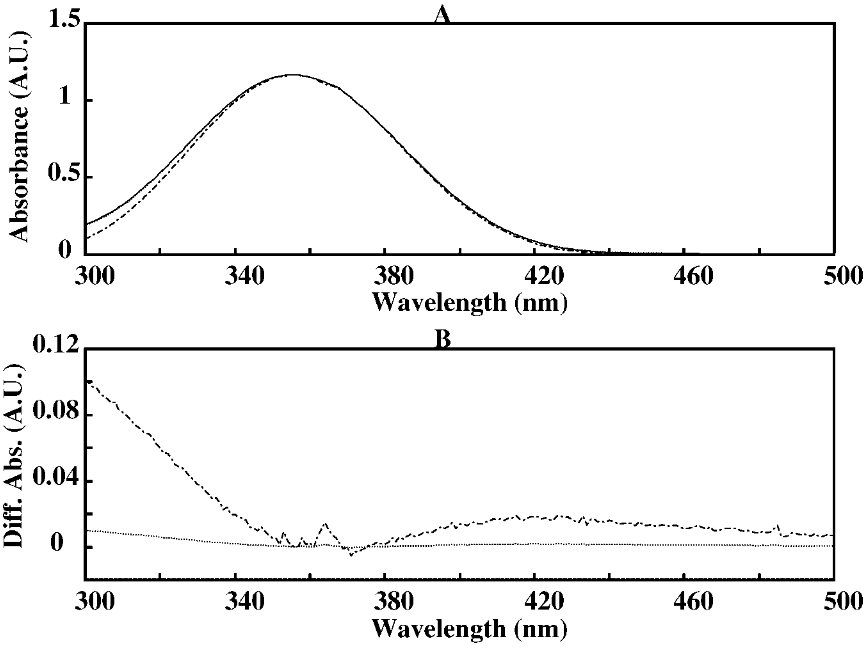

Figure 2. A. Imposed spectra of reactant without shape differences (full line), with realistic shape differences (dotted line) and with large shape differences (broken line). B. Differences between imposed pure spectrum without shape differences and imposed pure spectra with realistic shape differences (dotted line) and large shape differences (broken line).

CCR, constraint R, constraint RP and constraint P (Figures 4A–4D respectively).

In general, it was expected that the use of constraints would always improve the precision of both reaction rate constant estimates as claimed in the literature [21–23]. It is possible that noise and shape differences in the imposed pure spectrum of the reactant are responsible for the poorer precision for k_2 in the case of constraint R compared to no constraints. In data matrix **A**, spectral information about the reactant is dominant compared to spectral information about the product. Therefore the imposed pure spectrum of the reactant should be of high quality.

The precision of the k_1 estimates obtained using uncon-

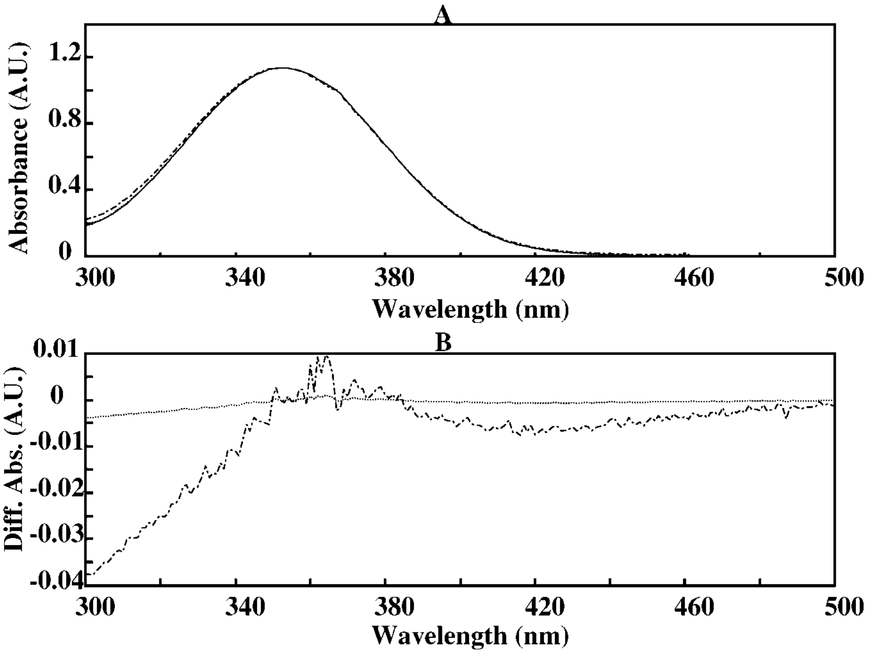

Figure 3. A. Imposed spectra of product without shape differences (full line), with realistic shape differences (dotted line) and with large shape differences (broken line). B. Differences between imposed pure spectrum without shape differences and imposed pure spectra with realistic shape differences (dotted line) and large shape differences (broken line).

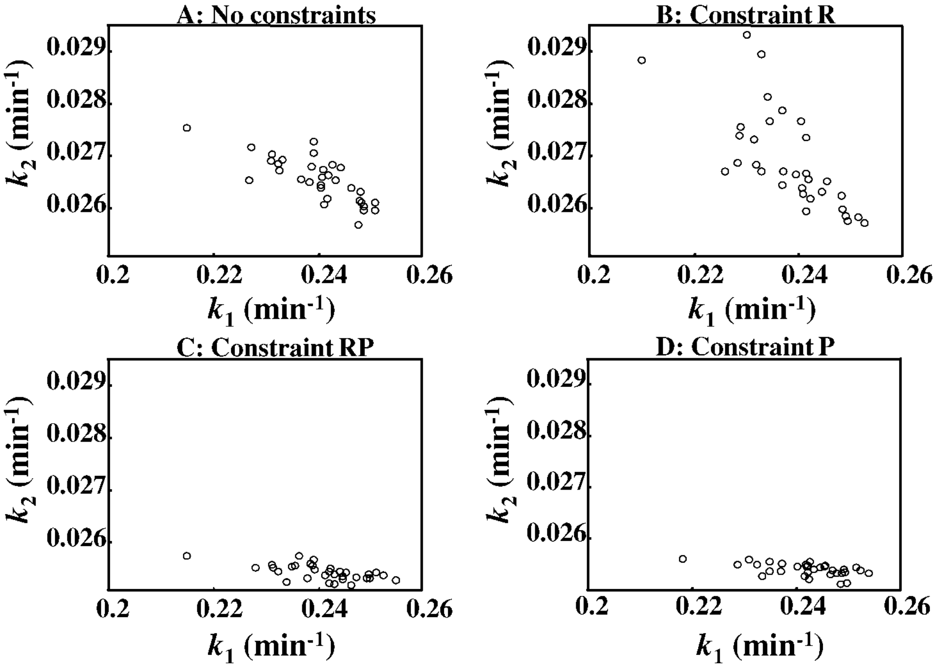

Figure 4. Individual reaction rate constant estimates using CCR.

strained and constrained CCR is approximately the same. Temperature fluctuations at the start of the reaction and/or initial concentration errors of the reactant might explain this result. These sources of variation mainly affect the first step of the reaction and hence the value of k_1. This extra variation in k_1 could easily mask the expected improvement in the precision of k_1 brought about by imposing a constraint.

Imposing constraint NNLS did not improve the precision of the reaction rate constant estimates. In NNLS, negative absorbances are not allowed. The noise level of the spectra taken in time of the reacting system is low, and hardly any negative absorbances are present. The non-negativity restriction will therefore not have much effect in this case.

4.1.2. Reconstruction error of the pure spectra

The pure spectra of the reactant and product and the CCR-estimated pure spectra are compared by calculating difference spectra. Representative difference spectra of the reactant and product are shown in Figure 5. In the case of constraint R, only the difference spectrum of the product can

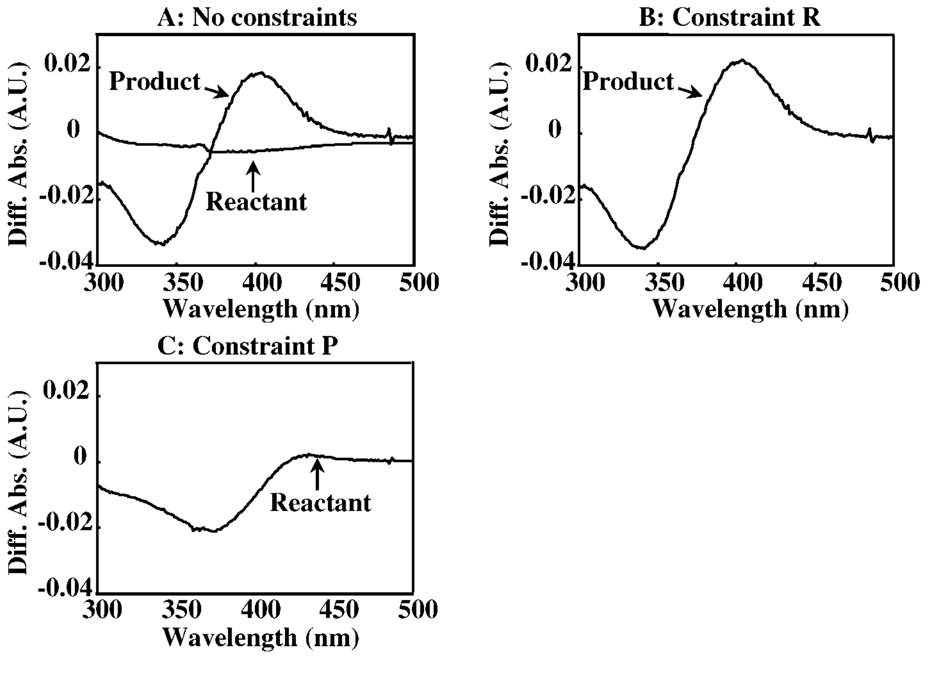

Figure 5. Difference spectra obtained for reactant and product using one individual batch.

Table I. Simulation results for different constraints (constr.) in the case of perfect *a priori* knowledge and two different noise levels. The relative error is indicated between parentheses in the columns of the accuracies

Constr.	Noise level (%)	Precision k_1 (10^{-9} (min^{-1})^2)	Precision k_2 (10^{-9} (min^{-1})^2)	Bias k_1 (10^{-9} (min^{-1})^2)	Bias k_2 (10^{-9} (min^{-1})^2)	Accuracy k_1 (10^{-9} (min^{-1})^2)	Accuracy k_2 (10^{-9} (min^{-1})^2)
None	0.2	20	3	< 1	< 1	20 (<1%)	3 (<1%)
R	0.2	12	3	< 1	< 1	12 (<1%)	3 (<1%)
P	0.2	7	< 1	< 1	< 1	7 (<1%)	< 1 (<1%)
RP	0.2	4	< 1	< 1	< 1	4 (<1%)	< 1 (<1%)
NNLS	0.2	20	3	< 1	< 1	20 (<1%)	3 (<1%)
None	2	1973	257	1	< 1	1974 (<1%)	257 (<1%)
R	2	1169	227	7	1	1176 (<1%)	228 (<1%)
P	2	588	3	< 1	< 1	588 (<1%)	3 (<1%)
RP	2	345	3	2	< 1	347 (<1%)	3 (<1%)
NNLS	2	1383	150	1030	162	2413 (<1%)	312 (2%)

be calculated, whereas for constraint P, only the difference spectrum of the reactant can be calculated. From Figure 5 the following can be observed.

1. The order of magnitude of all difference spectra is small compared to the original spectra (maximum absorbance 1.2 AU); see Figure 1. Yet, some structure is still present in the difference spectra of the product (Figures 5A and 5B).
2. For unconstrained CCR the difference spectrum of the reactant is smaller than the difference spectrum of the product (Figure 5A).
3. The difference spectrum of the product is comparable for unconstrained CCR and constraint R (Figures 5A and 5B).
4. The order of magnitude of the difference spectrum of the reactant for unconstrained CCR and constraint P differs (Figures 5A and 5C).

The difference spectrum of the reactant is smaller than the difference spectrum of the product (Figure 5A). This may again be attributed to the dominance of the spectral information of the reactant, which allows a better CCR estimate of the reactant spectrum from the available mixture spectra. It was expected that a poorer precision of reaction rate constant estimates would correspond also to a poorer precision of pure spectra estimates. However, if the precision of the reaction rate constant estimates becomes poorer— compare CCR using constraint R (Figure 4B) with unconstrained CCR (Figure 4A) — this does not correspond to an increased difference spectrum of the product (compare Figures 5A and 5B).

The individual estimates of the intermediate spectrum show very small shape differences. If the precision of the k_2 estimates becomes poorer, this is probably compensated by shape differences in the intermediate pure spectra estimates.

4.1.3. *Spectral residuals*

The root mean sum of squares of residuals was equal to 1.6×10^{-4} AU (no constraints), 2.9×10^{-4} AU (constraint R), 29×10^{-4} AU (constraint P) and 32×10^{-4} AU (constraint RP). The root mean sum of squares of the spectral noise level is equal to 1.9×10^{-4} AU. From these values it can be concluded that hardly any overfitting occurs.

4.2. Simulations

4.2.1. *Precision, bias and accuracy of reaction rate constant estimates: perfect a priori knowledge*

Table I shows the results for perfect *a priori* knowledge. From Table I the following can be observed.

Precision

1. For both noise levels the best precision of both reaction rate constant estimates is obtained using constraint RP.
2. For both noise levels the precision of the k_1 estimates obtained using constraint R is slightly better than the results obtained in the case of no constraints. The precision of the k_2 estimates is similar for constraint R and no constraints.
3. For both noise levels the precision of the k_1 estimates obtained using constraint RP is slightly better than the results obtained in the case of constraint P. The precision of the k_2 estimates is similar for constraint RP and constraint P.
4. Imposing the NNLS constraint leads to a slight improvement in the precision of both reaction rate constant estimates only for a noise level of 2%.

Bias

1. For both noise levels there is no bias present in the case of unconstrained CCR.
2. Imposing the NNLS constraint leads to a large bias (approximately a factor of 1000 for k_1 and a factor of 160 for k_2) of reaction rate constant estimates compared to unconstrained CCR for a noise level of 2%.

Accuracy

1. The best accuracy of both reaction rate constant estimates is obtained using constraint RP. This holds for both noise levels.
2. For both noise levels the accuracy of the k_1 estimates obtained using constraint R is better than the results obtained in the case of no constraints. The accuracy of the k_2 estimates is similar for constraint R and no constraints.
3. For both noise levels the accuracy of the k_1 estimates

Table II. Simulation results for different constraints (constr.) in the case of imperfect *a priori* knowledge and two different noise levels. Noise has been added to the pure spectra in the case of the use of constraints. The relative error is indicated between parentheses in the columns of the accuracies

Constr.	Noise level (%)	Precision k_1 (10^{-9} (min^{-1})^2)	Precision k_2 (10^{-9} (min^{-1})^2)	Bias k_1 (10^{-9} (min^{-1})^2)	Bias k_2 (10^{-9} (min^{-1})^2)	Accuracy k_1 (10^{-9} (min^{-1})^2)	Accuracy k_2 (10^{-9} (min^{-1})^2)
None	0.2	20	3	< 1	< 1	20 (<1%)	3 (<1%)
R	0.2	3830	186	6090	760	9920 (1%)	946 (3%)
P	0.2	230	22	1426	38	1656 (<1%)	60 (1%)
RP	0.2	1630	26	10052	105	11682 (1%)	131 (1%)
None	2	1973	257	1	< 1	1974 (<1%)	257 (<1%)
R	2	4657	382	6484	768	11141 (1%)	1150 (3%)
P	2	985	28	1318	39	2303 (1%)	67 (1%)
RP	2	2316	27	10182	109	12498 (1%)	136 (1%)

obtained using constraint RP is better than the results obtained in the case of constraint P. The accuracy of the k_2 estimates is similar for constraint RP and constraint P.

4. For a noise level of 2%, imposing the NNLS constraint leads to a slightly poorer accuracy of reaction rate constant estimates compared to the results obtained in the case of no constraints.

In general, the use of perfect *a priori* spectral knowledge is beneficial with respect to the precisions and accuracies of reaction rate constant estimates. The only exception is constraint NNLS. The best precision/accuracy of reaction rate constant estimates is obtained for constraint RP. For constraint R the precision/accuracy for k_1 is better than imposing no constraints and worse than imposing constraint RP.

Matrix **A** contains less information about the product (low selectivity in the time direction) compared to the reactant, and there is a large overlap present between the pure spectra of the reactant and product (low selectivity in the wavelength direction). Hence imposing constraint RP or constraint P will result in a large gain in precision/accuracy of reaction rate constant estimates, especially for k_2, because the product is mainly determined by k_2.

A noise level of 2% on the **A** matrix results in a large bias if constraint NNLS is imposed. The considerable amount of negative absorbances in the simulated mixture spectra at this noise level and the fact that negative absorbances are not allowed in NNLS explain this. This means that an offset is introduced in the fitted spectral data, which may result in a bias depending on the order of magnitude of the offset.

4.2.2. Precision, bias and accuracy of reaction rate constant estimates: imperfect a priori knowledge

Table II shows the results for imperfect *a priori* knowledge. The imposed pure spectra of the reactant and product were disturbed by noise. From Table II the following can be observed.

Precision

1. For a noise level of 0.2% the use of constraint R, constraint P or constraint RP leads to a poorer precision of reaction rate constant estimates compared to the precision in the case of unconstrained CCR.
2. For both noise levels the use of constraint P and constraint RP gives a better precision of reaction rate constant estimates compared to the precision obtained for constraint R.
3. For a noise level of 2% the precision of both k_1 and k_2 estimates is improved using constraint P compared to unconstrained CCR.
4. For a noise level of 2%, constraint R leads to a poorer precision of both k_1 and k_2 estimates compared to no constraints.
5. For a noise level of 2%, constraint RP leads to a poorer precision of k_1 estimates and a better precision of k_2 estimates compared to unconstrained CCR.

Bias

1. In all cases a large bias (≥1%) is obtained compared to unconstrained CCR.
2. For both noise levels the use of constraint R has led to a smaller bias for k_1 compared to the bias for k_1 in the case of constraint RP. The opposite is observed for k_2.
3. For the two noise levels used, the bias of reaction rate constant estimates is almost independent of the noise levels.

Accuracy

1. For a noise level of 0.2% the use of constraint R, constraint P or constraint RP leads to a poorer accuracy of reaction rate constant estimates compared to the accuracy in the case of unconstrained CCR.
2. For both noise levels the use of constraint RP only gives a better accuracy of k_2 compared to the accuracy obtained for constraint R.
3. For both noise levels the use of constraint R has led to an extremely poor accuracy of the reaction rate constant estimates compared to the accuracy in the case of unconstrained CCR.
4. For a noise level of 2% the accuracy is improved for the k_2 estimates if constraint RP or constraint P is used compared to unconstrained CCR.

In most cases, imposing constraints with imperfect *a priori* knowledge, i.e. adding noise (both noise levels) to the imposed spectra, must be avoided. However, there are exceptions. The precision and accuracy of the k_2 estimates are

Table III. Simulation results for different constraints (constr.) in the case of imperfect *a priori* knowledge and two different noise levels. Realistic (r) or large (l) shape differences have been introduced in the pure spectra in the case of the use of constraints. The relative error is indicated between parentheses in the columns of the accuracies

Constr.	Noise level (%)	Precision k_1 (10^{-9} $(\text{min}^{-1})^2$)	Precision k_2 (10^{-9} $(\text{min}^{-1})^2$)	Bias k_1 (10^{-9} $(\text{min}^{-1})^2$)	Bias k_2 (10^{-9} $(\text{min}^{-1})^2$)	Accuracy k_1 (10^{-9} $(\text{min}^{-1})^2$)	Accuracy k_2 (10^{-9} $(\text{min}^{-1})^2$)
None	0.2	20	3	< 1	< 1	20 (<1%)	3 (<1%)
R (r)	0.2	13	3	1	< 1	14 (<1%)	4 (<1%)
R (l)	0.2	12	2	20134	1541	20146 (2%)	1543 (5%)
P (r)	0.2	7	< 1	2	< 1	9 (<1%)	<1 (<1%)
P (l)	0.2	7	< 1	13	1	20 (<1%)	1 (<1%)
RP (r)	0.2	4	< 1	< 1	< 1	4 (< 1%)	1 (< 1%)
RP (l)	0.2	3	< 1	16118	83	16121 (2%)	83 (1%)
None	2	1973	257	1	< 1	1974 (<1%)	257 (2%)
R (r)	2	1299	256	10	< 1	1309 (< 1%)	256 (2%)
R (l)	2	1253	239	19865	1479	21118 (<1%)	1718 (5%)
P (r)	2	680	3	8	< 1	688 (<1%)	3 (<1%)
P (l)	2	672	3	3	2	675 (<1%)	5 (<1%)
RP (r)	2	398	3	2	< 1	400 (< 1%)	3 (< 1%)
RP (l)	2	404	3	16148	84	16552 (2%)	87 (1%)

improved if a high noise level is present in the data and pure spectra (RP or P is imposed), despite the presence of biased estimates. This is probably caused by the fact that data matrix **A** contains less information about the product compared to the reactant. The accuracy of reaction rate constant estimates obtained is independent of the two noise levels used.

Table III shows the simulation results using imperfect *a priori* knowledge with realistic or large shape differences in the pure imposed spectra of the reacting absorbing species. From Table III the following can be observed.

Precision

1. For both noise levels the use of constraint RP gives the best precision of reaction rate constant estimates compared to the precision using constraint R, constraint P or no constraint.
2. If for both noise levels the precision of reaction rate constant estimates for constraint R, constraint P and constraint RP (Table III) for realistic and large shape differences is compared to the precision obtained for these constraints in Table I (perfect *a priori* knowledge), it is obvious that they are similar.

Bias

1. In the case of large shape differences a large bias ($\geq$1%) is obtained for both noise levels using constraint R and constraint RP.
2. For both noise levels used, no large bias is obtained in the case of constraint P and large shape differences.
3. The order of magnitude of the bias of reaction rate constant estimates is independent of the two noise levels used.

Accuracy

1. In the case of large shape differences a poor accuracy of reaction rate constants is obtained in the case of constraint R and constraint RP.
2. For a noise level of 0.2% and large shape differences the accuracy of the k_2 estimates is improved using constraint P compared to unconstrained CCR. The accuracy of the k_1 estimates is similar.
3. For a noise level of 2% and large shape differences the accuracy of both the k_1 and k_2 estimates is improved using constraint P compared to unconstrained CCR.

It is obvious that imperfect *a priori* knowledge by means of introducing realistic or large shape differences in the pure spectra has no effect on the precision of the reaction rate constant estimates. However, for large shape differences using constraint R and constraint RP, a large bias and poor accuracy of reaction rate constant estimates are obtained independently of the noise level. Again the dominance of the spectral information about the reactant in the data set explains this.

In the case of constraint P and large shape differences, no biased estimates are obtained. Moreover, for a high noise level and large shape differences the accuracy is improved using constraint P compared to unconstrained CCR, because less information of the product is present in data matrix **A** compared to the reactant.

If realistic shape differences are introduced, which are representative of the experiments performed, the precision, bias and accuracy are not affected compared to the corresponding cases for perfect *a priori* knowledge.

4.2.3. *Summary of the simulation results*

Precision and accuracy

In the case of perfect *a priori* knowledge, applying constraints leads to a better precision and accuracy of reaction rate constant estimates. If noise is added to the imposed pure spectra, which results in imperfect *a priori* knowledge, the precision and accuracy of reaction rate constant estimates

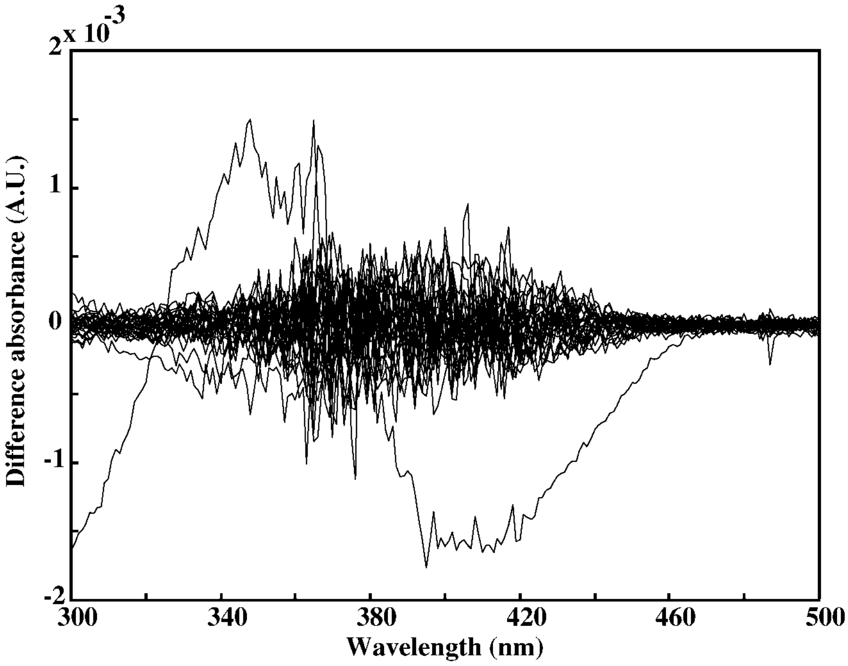

Figure 6. Spectral residuals of one individual batch process using unconstrained CCR. The spectral residuals have been plotted using an interval of 10 residual spectra.

become poorer. However, there are exceptions. In the case of a high noise level, imposing constraint RP or constraint P may improve the precision and accuracy of reaction rate constant estimates. If imperfect knowledge is present in the form of realistic or larger shape differences in the pure spectra, the precision of reaction rate constant estimates is similar to that obtained in the case of perfect *a priori* knowledge. A poor accuracy of reaction rate constant estimates is obtained in the case of large shape differences. However, in the case of large shape differences and imposing constraint P, the accuracy is improved compared to unconstrained CCR.

Bias

In the case of a high noise level and perfect *a priori* knowledge, imposing the NNLS constraint gives a large bias for both reaction rate constant estimates owing to negative absorbances present in the spectral data. If imperfect *a priori* knowledge is used (noise or large shape differences added to imposed pure spectra), a large bias of reaction rate constant estimates can be obtained. However, for a high noise level, no bias is obtained in the case of constraint P and large shape differences. The order of magnitude of the bias of reaction rate constant estimates is independent of the two noise levels imposed on the pure spectra in this study. No bias is obtained in the case of realistic shape differences introduced in the imposed pure spectra.

4.2.4. Spectral residuals

For the results of the simulations, spectral residuals have been inspected. In all cases (perfect and imperfect *a priori* knowledge) the spectral residuals represented white noise, except for imperfect *a priori* knowledge where large shape differences have been introduced in the pure spectra. Hence it might be claimed that structure in the residuals is an indication of the quality of the *a priori* incorporated spectra with respect to the shape.

In Figure 6 the spectral residuals are shown for one batch process of the experimental data set in the case of unconstrained CCR. The two largest spectral residual spectra are the first two spectral residual spectra of the batch process. The spectral residuals for other batches were similar. The residuals show some structure, which can be caused by spectral characteristics such as drift, non-uniform errors and colored noise. Hence spectral residuals are not good indicators of the quality of the *a priori* imposed pure spectra, because in the residuals of unconstrained CCR there is already structure present. In the case of unconstrained CCR a comparison of pure spectra estimates and measured pure spectra can serve as a diagnostic tool. If there are large differences between the pure spectra estimates and the measured pure spectra, imposing the measured pure spectra may cause biased reaction rate constant estimates.

4.2.5. Bias of NNLS

For a noise level of 2%, k_1 and k_2 were estimated using no constraints and constraint NNLS for one particular simulated UV-vis data set. Next a grid of k_1 and k_2 values was chosen around the optimal values found. For every combination of k_1 and k_2 grid values the concentration profiles were reconstructed and the pure spectra involved were estimated. Finally, the sum of squares of the spectral residuals was calculated for every combination of k_1 and k_2 grid values. Now it is possible to make contour plots which show lines of constant sums of squares. Figure 7 shows the contour plots obtained in the case of no constraint and in the case of constraint NNLS. The optimal values found for the

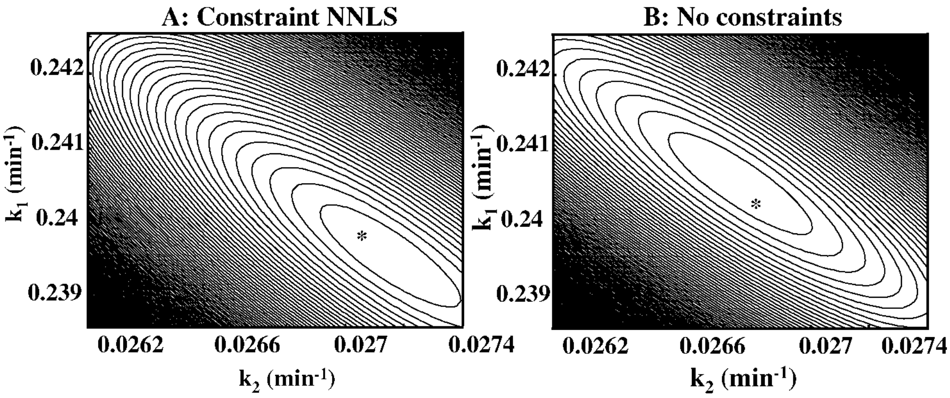

Figure 7. Contour plots of sum of squares of spectral residuals obtained using a simulated data set and a grid of k_1 and k_2 values. The reaction rate constant estimates found in these particular cases are indicated by asterisks.

reaction rate constants are also plotted in the same figure as asterisks. It is obvious that approximately the real minimum has been found in both cases. The contour lines in Figures 7A and 7B are different, because in the case of constraint NNLS, parts of the cross-section of the total error surface are not accessible. This can lead to a large bias of reaction rate constant estimates if negative absorbances are present in the spectral data. This issue will play a more dominant role if the noise level of the spectral data is increased.

4.2.6. *Guidelines for using constraints*

From the experiments and simulations, guidelines can be formulated for using constraints with respect to the accuracy of reaction rate constant estimates valid for the kinetic system discussed in this paper. If the measured spectra contain no local regions in the time direction where only one species is dominantly present (no selectivity in the time direction) and the quality of the constraints is high, it is recommended to use these constraints. This holds especially if the reacting absorbing species have a poor spectral selectivity in the wavelength direction. If the measured spectra contain local regions in the time direction where only one species is dominantly present (selectivity in the time direction), it is better to use unconstrained models even in the case of a low selectivity in the wavelength direction for this species.

Table IV gives a general overview which may guide the application of constraints in CCR for a large spectral overlap of the reactant and product species. The criterion used is the accuracy of reaction rate constant estimates. For the kinetic system considered in this paper, the reactant is the dominant species in the time direction and the product is the non-dominant species in the time direction. A large overlap is present between the pure spectra of the reactant and product. Table IV summarizes the following results.

1. Consider the perfect *a priori* knowledge case from Table IV (see also Table I) for the dominant species in the time direction (reactant). It is useful to apply constraints concerning this species, because a gain in accuracy of reaction rate constant estimates is obtained if constraint R or constraint RP is implemented. In the case of the non-dominant species in the time direction (product) it is very useful to implement constraints concerning this species (constraint P or constraint RP).
2. For the dominant species it is very harmful to apply constraints for the imperfect *a priori* knowledge (noise) case (see also Table II). For the non-dominant species it is sometimes useful to apply imperfect constraints.
3. For realistic shape differences (see also Table III) it is useful to apply constraints for both types of species (constraint R, constraint RP, constraint P), especially for the non-dominant species (constraint RP and constraint P).
4. In the case of large shape differences (see also Table III) present in imposed pure spectra it is not useful to apply constraints at all. However, for a high noise level and the non-dominant species it is sometimes useful to apply constraint P in the case of large shape differences.

In practice, perfect *a priori* knowledge is never available.

Table IV. Overview of the use of constraints with respect to the accuracy of reaction rate constant estimates in the case of the presence of a dominant or a non-dominant species in the time direction and a large spectral overlap of this species with another species present: very useful (++), useful (+), sometimes useful (+/−), harmful (−), very harmful (−−)

Type of *a priori* knowledge	Dominant species in time direction	Non-dominant species in time direction
Perfect *a priori* knowledge	+	++
Imperfect *a priori* knowledge (noise)	−−	+/−
Imperfect *a priori* knowledge (realistic shape differences)	+	++
Imperfect *a priori* knowledge (large shape differences)	−−	+/−

Hence imposed pure spectra will suffer from realistic shape differences and noise. From the simulations it is obvious that the presence of realistic shape differences will not affect the precision and accuracy. However, imposing noisy spectra may lead to a poor precision and accuracy of reaction rate constant estimates. Also biased estimates can be obtained. Therefore in practice it is useful to measure the imposed pure spectra often in order to reduce the noise level. The alternative is to apply unconstrained CCR.

4.3. Comparison between experimental and simulation results

As mentioned earlier, a noise level of 0.2% in the simulated data is comparable to the level of instrumental noise present in the experiments. If the simulation results for this noise level and the precision of the reaction rate constant estimates for the experimental data are considered, the following can be observed.

1. Imposing constraint R on the experimental data leads to a poorer precision of the k_2 estimates compared to the results obtained for no constraints. The precision of the k_1 estimates is similar for constraint R and unconstrained CCR. It is assumed that unconstrained CCR gives unbiased estimates as was concluded from the simulations. Therefore biased estimates are obtained in the case of constraint R for k_2. A poorer precision of k_2 in the case of constraint R can be caused by the presence of noise on the imposed pure spectra. The k_1 estimates are similar in the case of constrained CCR and unconstrained CCR, suggesting that the main error sources that possibly affect the estimates are the temperature fluctuations at the start of the reaction and initial concentration errors.
2. The use of constraint RP or constraint P gives a clear gain in precision of k_2 estimates for the experimental data. However, probably biased estimates are obtained as can be seen from the results of the simulated data. The precision of the k_1 estimates is similar for constrained and unconstrained CCR. It is also obvious from the simulated data that applying constraint RP or constraint P improves the accuracy of reaction rate constant estimates, especially for k_2.

5. CONCLUSION

In this paper the usefulness of constraints for improving the accuracy of rate constant estimates from kinetic data has been investigated. From the UV-vis measurements of a two-step consecutive biochemical reaction performed under pseudo-first-order conditions, it can be concluded that the precision of the reaction rate constant estimates is best if the *a priori* known pure spectra of the reactant and product or the *a priori* known pure spectrum of the product are implemented as constraints in classical curve resolution (CCR). A large overlap is present between the pure spectra of the reactant and product. The presence of biased estimates of reaction rate constants could not be checked, but was suspected to be present assuming that no biased estimates are obtained in the case of unconstrained CCR.

In order to investigate whether biased reaction rate constant estimates are obtained using CCR with and without constraints implemented, simulations have been set up so that the simulated UV-vis spectra look very similar to the experimental spectra. Using perfect *a priori* knowledge improved the precisions and accuracies of reaction rate constant estimates. However, imposing noisy pure spectra (imperfect *a priori* knowledge) resulted in poor precisions and accuracies of reaction rate constant estimates. Moreover, a large bias of reaction rate constant estimates is obtained. However, in the case of imposing only a noisy pure spectrum of the product, the accuracy of reaction rate constants is improved compared to unconstrained CCR, despite the presence of biased estimates. In the case of imposing imperfect *a priori* knowledge by means of introducing large shape differences in the pure spectra, a large bias of reaction rate constants is obtained, but the precision is not affected. However, in the case of imposing only the pure spectrum of the product, the accuracy is improved compared to unconstrained CCR.

From the results of the simulated data, guidelines have been formulated for the use of constraints with respect to the accuracy of reaction rate constants valid for the kinetic system discussed in this paper. If the measured spectra contain no local regions in the time direction where only one species is dominantly present (low selectivity in the time direction) and the quality of the constraints is high, and there is no selectivity for this species in the wavelength direction, it is useful to impose the constraints. If the measured spectra contain local regions in the time direction where only one species is dominantly present (high selectivity in the time direction), it is better to use unconstrained models for this species.

In practice, a better precision obtained by imposing constraints is no good reason to use constraints. The true values of the reaction rate constants of interest are always unknown. This makes it difficult to check whether biased reaction rate constant estimates have been obtained. Some diagnostic tools are proposed.

APPENDIX CCR ALGORITHM

Initialization

Construct the estimate of $\mathbf{F}$, $\hat{\mathbf{F}}$, using Equations (2)–(4) from Section 2.2 and the starting values for k_1 and k_2.

Minimization of SSQ

Repeat step 1 to step 5 until SSQ has been minimized.

1. Minimize Equation (12) with respect to $\hat{\mathbf{D}}$, where $\hat{\mathbf{D}}$ is obtained using Equation (13) by means of an ordinary least squares step:

$$\min_{\hat{\mathbf{D}}} \left\| \mathbf{A} - \hat{\mathbf{D}}\hat{\mathbf{F}}^{\mathrm{T}} \right\|^2 \tag{12}$$

$$\hat{\mathbf{D}} = \mathbf{A}\hat{\mathbf{F}}(\hat{\mathbf{F}}^{\mathrm{T}}\hat{\mathbf{F}})^{-1} \tag{13}$$

2. Update the reaction rate constants using the Levenberg–

Marquardt [28] algorithm by solving

$$\min_{\hat{k}_1,\hat{k}_2} \left\| \mathbf{A} - \hat{\mathbf{D}}\hat{\mathbf{F}}^{\mathrm{T}} \right\|^2 \tag{14}$$

3. Calculate $\hat{\mathbf{A}}$ according to

$$\hat{\mathbf{A}} = \hat{\mathbf{D}}\hat{\mathbf{F}}^{\mathrm{T}} \tag{15}$$

4. Calculate matrix $\mathbf{E}$ by applying

$$\mathbf{E} = \mathbf{A} - \hat{\mathbf{A}} \tag{16}$$

5. Calculate SSQ.

It is important to stress that *all* concentration profiles of $\hat{\mathbf{F}}$ are updated simultaneously in *every* iteration.

REFERENCES

1. Furusjö E, Danielsson L-G. Target testing procedure for determining chemical kinetics from spectroscopic data with absorption shifts and baseline drift. *Chemometrics Intell. Lab. Syst.* 2000; **50**: 63–73.
2. Bugnon P, Chottard J-C, Jestin J-L, Jung B, Laurenczy G, Maeder M, Merbach AE, Zuberbühler AD. Second-order globalisation for the determination of activation parameters in kinetics. *Anal. Chim. Acta* 1994; **298**: 193–201.
3. Maeder M, Molloy KJ, Schumacher MM. Analysis of non-isothermal kinetic measurements. *Anal. Chim. Acta* 1997; **337**: 73–81.
4. Molloy KJ, Maeder M, Schumacher MM. Hard modelling of spectroscopic measurements. Applications in non-ideal industrial reaction systems. *Chemometrics Intell. Lab. Syst.* 1999; **46**: 221–230.
5. Jimenez-Prieto R, Velasco A, Silva M, Perez-Bendito D. Kalman filtering of data from first- and second-order kinetics. *Talanta* 1993; **40**: 1731–1739.
6. Mok K-W, Chau F-T. Application of the extended Kalman filter for analysis of a consecutive first-order reaction. *Trends Anal. Chem.* 1996; **15**: 170–174.
7. Drobnica L, Sturdik E. The reaction of carbonyl cyanide phenylhydrazones with thiols. *Biochim. Biophys. Acta* 1979; **585**: 462–476.
8. Bisby RH, Thomas EW. Kinetic analysis by the method of nonlinear least squares. *J. Chem. Educ.* 1986; **63**: 990–992.
9. Chrastil J. Determination of the first order consecutive reaction rate constants from final product. *Comput. Chem.* 1988; **12**: 289–292.
10. Chau F-T, Mok K-W. Multiwavelength analysis for a first-order consecutive reaction. *Comput. Chem.* 1992; **16**: 239–242.
11. Chrastil J. Determination of the first order consecutive reversible reaction kinetics. *Comput. Chem.* 1993; **17**: 103–106.
12. Bijlsma S, Boelens HFM, Hoefsloot HCJ, Smilde AK. Estimating reaction rate constants: comparison between traditional curve fitting and curve resolution. *Anal. Chim. Acta* 2000; **419**: 197–207.
13. Sylvestre EA, Lawton WH, Maggio MS. Curve resolution using a postulated chemical reaction. *Technometrics* 1974; **16**: 353–368.
14. Bijlsma S, Louwerse DJ, Smilde AK. Rapid estimation of rate constants of batch processes using on-line SW-NIR. *AIChE J.* 1998; **44**: 2713–2723.
15. Bijlsma S, Smilde AK. Application of curve resolution based methods to kinetic data. *Anal. Chim. Acta* 1999; **396**: 231–240.
16. Bijlsma S, Smilde AK. Estimating reaction rate constants from a two-step reaction: comparison between two-way and three-way methods. *J. Chemometrics* 2000; **14**: 541–560.
17. Bijlsma S, Boelens HFM, Smilde AK. Rapid determination of rate constants in second-order kinetics using UV-vis spectroscopy. *Applied Spectroscopy*, accepted September 2000.
18. Bijlsma S, Louwerse DJ, Windig W, Smilde AK. Rapid estimation of rate constants using on-line SW-NIR and trilinear models. *Anal. Chim. Acta* 1998; **376**: 339–355.
19. Bijlsma S, Louwerse DJ, Smilde AK. Estimating rate constants and pure UV-vis spectra of a two-step reaction using trilinear models. *J. Chemometrics* 1999; **13**: 311–329.
20. Lawton WH, Sylvestre EA. Self modeling curve resolution. *Technometrics* 1971; **13**: 617–633.
21. Tauler R, Smilde A, Kowalski B. Selectivity, local rank, three-way data analysis and ambiguity in multivariate curve resolution. *J. Chemometrics* 1995; **9**: 31–58.
22. De Juan A, van der Heyden Y, Tauler R, Massart DL. Assessment of new constraints applied to the alternating least squares method. *Anal. Chim. Acta* 1997; **346**: 307–318.
23. Saurina J, Hernandez-Cassou S, Tauler R. Multivariate curve resolution and trilinear decomposition methods in the analysis of stopped-flow kinetic data for binary amino acid mixtures. *Anal. Chem.* 1997: **69**: 2329–2336.
24. Bro R, de Jong S. A fast non-negativity-constrained least squares algorithm. *J. Chemometrics* 1997; **11**: 393–402.
25. Burns DA, Ciurczak EW. *Handbook of Near-infrared Analysis*, Dekker: New York, 1992.
26. Vajada S, Rabitz H. Identifiability and distinguishability of first-order reaction systems. *Phys. Chem.* 1988; **92**: 701–707.
27. Vajada S, Rabitz H. Identifiability and distinguishability of general reaction systems. *J. Phys. Chem.* 1994; **98**: 5265–5271.
28. Press WH, Teukolsky SA, Vetterling WT, Flannery BP. *Numerical Recipes*. Cambridge University Press: New York, 1992.